View metadata, citation and similar papers at core.ac.uk
brought to you by CORE
provided by Xiamen University Institutional Repository

Journal of
Materials Chemistry C

RSC Publishing

PAPER

View Article Online
View Journal | View Issue

Published on 04 September 2013. Downloaded by Xiamen University on 12/07/2015 08:24:29.

Self-mask fabrication of uniformly orientated SiGe island/SiGe/Si hetero-nanowire arrays with controllable sizes

Cite this: *J. Mater. Chem. C*, 2013, **1**, 6878

Dongfeng Qi, Hanhui Liu, Wei Gao, Qinqin Sun, Songyan Chen,* Wei Huang, Cheng Li and Hongkai Lai

Received 9th July 2013
Accepted 4th September 2013

DOI: 10.1039/c3tc31306a

www.rsc.org/MaterialsC

We report the synthesis of SiGe island/SiGe/Si hetero-nanowire arrays using laser-induced SiGe islands as templates followed by Ar ion beam etching (IBE). Firstly, single crystal SiGe islands with an average aspect ratio of 0.96 are prepared by pulse laser irradiation of amorphous Ge film on Si substrate. It is interesting to note that these SiGe islands can serve as masks, and uniformly orientated SiGe island/SiGe/Si nanowires can be fabricated by Ar IBE. Moreover, the diameters of the hetero-nanowires can be well-controlled by the size of the SiGe islands determined by the energy density of the pulse laser during the crystallization. Our experiments show the unique nonlithographic self-mask method and demonstrate the mass production of SiGe island/SiGe/Si hetero-nanowire arrays which may find applications in nanodevices.

1. Introduction

Arrays of Si nanowires (NWs) and SiGe/Si heterostructures are attracting intensive research interest because of their potential usage in semiconductor technology,[1,2] advanced electronic devices,[3,4] optical devices,[5,6] biological/chemical sensors,[7,8] and renewable energy devices. The controllable fabrication of Si-based nanowires is a prerequisite for their application in devices. Consequently, numerous methods have been developed to fabricate small and controllable Si-based nanostructures based on the top-down approach, such as ion beam etching, reactive ion etching (RIE), or metal-assisted chemical etching.[9–15] However, it is noted that these etching methods always result in randomly oriented Si NWs with a broad distribution of diameter and length.

Moreover, for Si nanowire devices, an important issue that we urgently need to overcome is that of metal-free nanowires. However, all the Si-based NWs fabricated by the bottom up vapor–liquid–solid (VLS) method inevitably contain saturated dopants from the metal catalyst.[16–22] As is well-known to all, metal impurities in Si show serious problems of low yields and poor performances of devices due to induced detrimental effects,[23–26] for example, noble metal impurities will form deep level centers, which ultimately act as efficient generation recombination centers to increase the leakage current of junctions. Furthermore, masks without lethal impurities are an important parameter, especially for high-performance devices using uniform orientation nanowire arrays. Therefore, an ultra-clean Si wafer surface without metal impurities is essential to achieve high-performance devices. In this paper, we propose self-organized SiGe islands on a Si substrate as masks, which may open up a new path to achieve Si-based nanowires without metal impurities.

Besides the advantages of catalyst-free masks, self-organized SiGe or Ge islands with nanometer scales are expected to be utilized in future silicon-based optoelectronics devices and single-electron devices with high quantum efficiencies.[27–33] One challenge in this field is the fabrication of NWs with a high aspect ratio (AR). The aspect ratio (AR) is defined as the ratio of the height *versus* the square root of the island's base area. Many groups have investigated self-organized Ge islands grown on Si substrates *via* the Stranski–Krastanov growth mode.[34] Under different growth conditions, the Ge islands range from pyramid shapes[35] with AR = 0.1, to multi-faceted dome shapes[36] with AR = 0.2, and to barns with AR = 0.3.[37] The new "cupola" SiGe islands exhibit an aspect ratio as high as 0.38 and their shape approaches that of a multi-faceted half sphere.[38] Until now, abundant experimental results about the AR of SiGe islands are generally low, and no group has used self-organized SiGe or Ge islands as masks to fabricate Si-based nanowires. Differently from the low aspect ratio islands (pyramid, dome, barn and cupola), three dimensions of the size of the high aspect ratio islands are at 100 nm (nm) below, and the movement of electrons in the islands is subject to limitations, and quantum-confined in three of their dimensions.[39–41] With tailoring the band structure artificially with uniformly shaped islands and the three quantum confinement effect,[42–44] combined with

Department of Physics, Semiconductor Photonics Research Center, Xiamen University, 422 South Siming Road, Xiamen 361005, People's Republic of China. E-mail: sychen@xmu.edu.cn

This journal is © The Royal Society of Chemistry 2013

Published on 04 September 2013. Downloaded by Xiamen University on 12/07/2015 08:24:29.

modulated-doping and carrier filling effect, high efficiency light-emitting Si-based nano-Ge/SiGe heterostructures are expected, which may be beneficial for the monolithic integration of Si-based photonic devices. In point of realizing, making use of the technique of top-down etching to combine the self-organized islands with Si-based nanowires, exerts each of these advantages. If these uniform distribution islands can be used as masks, they may provide an effective way to fabricate catalyst-free NWs. As well, the high quantum efficiencies of the islands[28–30] could also be incorporated into the Si NWs[1–4] to fabricate high-performance single-electron devices or SiGe/Si nanowire heteronanocrystals memory structures in the future. However, the aspect ratio of the self-organized islands that grow in the traditional Stranski–Krastanov growth mode is low, so these islands neither have high quantum efficiencies, nor can act as masks.

In order to overcome these difficulties, here we demonstrate a new nonlithographic technique to synthesize SiGe island/SiGe/Si NW arrays on a Si (100) substrate with well-defined diameters and uniform orientation. The SiGe islands with a high AR (0.96 as average) were obtained by pulse laser irradiation. These SiGe islands are perfect single crystals in nature and their size can be tuned *via* changing the incident laser energy. Using the SiGe islands as masks, ordered arrays of SiGe island/SiGe/Si nanowires without metal impurities are fabricated after high-energy Ar IBE. These SiGe islands/Si nanowire structures may open up new perspectives for applications in nano-electronics and optoelectronics.

2. Experimental

Fig. 1 depicts a schematic diagram of the mask-free fabrication of the SiGe island/SiGe/Si NWs. In Process 1, 4 inch n-type Si (100) wafers with a resistivity of 0.1–1 Ω cm were used as the substrates. They were firstly cleaned by an RCA (Radio Corporation of America) method and dried by N_2 before loading into a cold-wall ultrahigh vacuum chemical vapor deposition (UHV/CVD) system with a base pressure of 5×10^{-8} Pa. The wafers were baked at 850 °C for 30 min to de-oxidise. Then a 20 nm-thick low temperature Ge (LT-Ge) film was evaporated on the n-type Si (100) substrate from a Knudsen effusion cell source which contains solid Ge with a purity of 99.999%. During the evaporation, the cell was heated to 1100 °C, the Si substrate temperature was maintained at 180 °C and was rotated during deposition to assure a homogeneous Ge coverage.

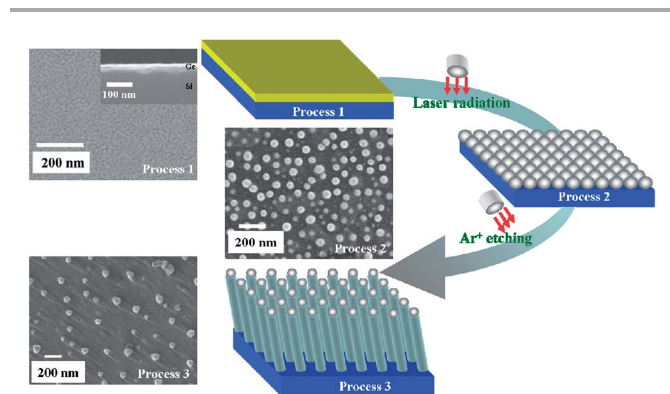

Fig. 1 Preparation process of the SiGe island/SiGe/Si nanowires. Process 1: 20 nm amorphous Ge film was grown on the Si substrate. Process 2: transformation from Ge film to SiGe islands by laser radialization. Process 3: 30° tilted SiGe island/SiGe/Si nanowires were formed after Ar ion beam etching.

In the next step, a KrF excimer laser which operates at a wavelength of 248 nm with 25 ns pulse width and a 5 Hz repetition rate was used. A top flat beam profile of 5 mm × 8 mm was obtained to ensure uniform irradiation of the laser. The laser energy densities were tuned using a metallic neutral density filter. All experiments were performed in ambient nitrogen to avoid oxidation. After laser irradiation, uniform SiGe islands coupled with a graded SiGe inter-layer were created on the Si substrate. The morphologies of the formed surface structures were characterized by a scanning electron microscopy system (SEM, LEO 1530, with an operating voltage of 20 kV). The crystal quality and the composition of the fabricated islands were characterized by transmission electron microscopy (TEM, FEI 200, with an operating voltage of 200 kV).

Subsequently, these high AR (0.96 as average) SiGe islands were used as masks to fabricate an ordered array of SiGe island/SiGe/Si nanowires on the Si (100) substrate with Ar IBE. The Ar ion beam is extensively used for surface cleaning and ion-assisted dry etching of semiconductors.[45–50] In order to prove that uniform orientation NWs can be created by the top-down approach, the mask was etched by the Ar ion beam at a 30° incident angle. The vacuum pressure was in the range of 10^{-8} torr prior to the Ar gas introduction, and then the Ar pressure was maintained at 10^{-6} torr during etching. The nominal etching rate for SiO_2 was about 30.3 nm min^{-1} at a 30° tilt incidence for a 3 kV Ar ion beam with a current of 15 mA.

3. Results and discussion

We quantified the structural perfection of the laser-induced islands. TEM reveals the morphology of the islands in detail in

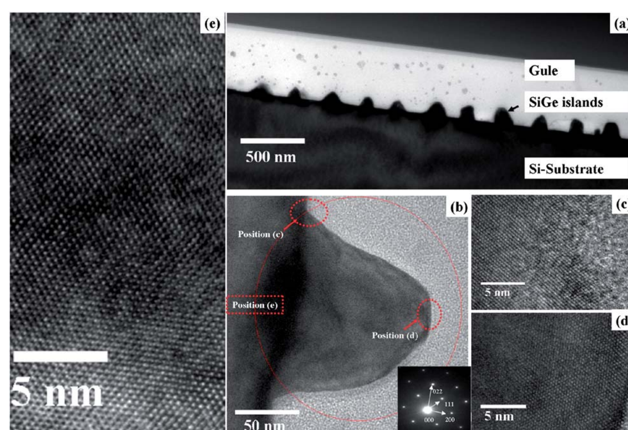

Fig. 2 TEM images of the island structures (with mean diameters of 80 nm). (a) Cross sectional TEM image of the SiGe alloy islands on a Si substrate; (b) cross sectional TEM image of a typical SiGe island. The inset image is the corresponding selected area electron diffraction image (which shows the single crystallinity of the SiGe island). (c)–(e) are HRTEM images showing the details in (b).

View Article Online

Published on 04 September 2013. Downloaded by Xiamen University on 12/07/2015 08:24:29.

Fig. 2. The low-magnification images in Fig. 2(a) show these special islands with an average AR of 0.96. Fig. 2b is a close-up image of an island. The inset image is the selected area electron diffraction (SAED) pattern of the island, whereas the SAED pattern confirms the [100] growth direction of the island, which is in accordance with the Si substrate. Fig. 2(c)–(e) show the high-resolution TEM (HRTEM) images of different positions in this island. The HRTEM images in Fig. 2(c) and (e) show that the island is single crystalline without obvious crystal defects, such as dislocations, while beneath the island, crystal defects do not exist either.

For further compositional analysis of the fabricated islands, the annular dark-field scanning TEM (ADF-STEM) and line profile of the EDS signal from the Si and Ge components of the island are presented in Fig. 3(b) and (c), respectively. The ADF-STEM (Fig. 3(c)) confirms the presence of a compositionally uniform Ge segment in the SiGe islands. STEM energy dispersive X-ray spectroscopy (EDS) line profiles (Fig. 3(c)) show that the composition transition occurs underneath the island, which is in agreement with the ADF analysis. This implies that the Ge component of the islands is uniform, and a graded SiGe interlayer (30 nm) is present beneath the island. Fig. 3(b) is the EDS line profile of Si and Ge through the adjacent island. The island has a high Ge component which is actually uniform in different islands, while the Ge component in the free areas is low.

Using the laser-induced high aspect ratio islands as masks, the SiGe island/SiGe/Si nanowires on the Si substrate can be fabricated by Ar IBE, as shown in Fig. 3(e). The NWs are packed in a density of 10^9 wires per cm^2. All have a uniform orientation which is corresponding to the 30° angel of the incident Ar ion beam and their diameters copied that of the islands. Each nanowire comprises of three segments: the tip SiGe island, the graded SiGe connection, and the Si stem. Due to the high aspect ratio islands, and the different Ge composition between islands and free area, the uniform composition SiGe islands masked substrates can be treated by Ar ion beam with 30° incident angel etching to form SiGe island/SiGe/Si nanowires with a uniform orientation on the Si substrate. No metals are used as catalysts, and this should prevent any saturated dopants from the catalyst. On the other hand, in chemical wet etching, the crystallographic orientation of the Si nanowires depends upon the diameter of the nanowires. Due to the existence of equivalent crystallographic directions, it is difficult to get epitaxial Si nanowires with uniform orientation relative to the surface of the Si substrate.[12,51] As a high-cost alternative method, obtaining nanowires with diameters smaller than 100 nm may be difficult, since there are limitations in achieving reliable diameter reduction by reactive ion etching (RIE) for the smaller dimensions.[52,53] In comparison with chemical wet etching or reactive ion etching techniques, the SiGe/Si hetero-nanowire with uniform orientation and small diameters can be formed by this method.

We have thus demonstrated for the first time the ability to use a laser-induced SiGe islands array as a masking template in the formation of SiGe island/SiGe/Si nanowires. This is of tremendous value since a careful manipulation of the size of the SiGe islands template will allow one to have control over the diameter of the nanowires without lethal impurities. Next, we change the energy density of the incident laser to obtain masks with different diameters. Fig. 4 shows the data of the SiGe islands diameters of different samples with laser energy densities ranging from 80 mJ cm^{-2} to 145 mJ cm^{-2}. The diameters can be widely tuned from 39.6 nm to a 148.9 nm depending on the laser energy density. The surface mean height was investigated by AFM, and which has the same variation tendency as the mean diameter. For different laser irradiated energies, the AR (height/diameter) of each island is about 0.61, 0.85, 1.01 and 0.81, respectively. Based on these results we know that the AR of each laser-induced island is large (AR > 0.61), and a larger diameter is coupled with a larger height, which can act as the best masks and provide the best nanowires. Panels (a)–(d)

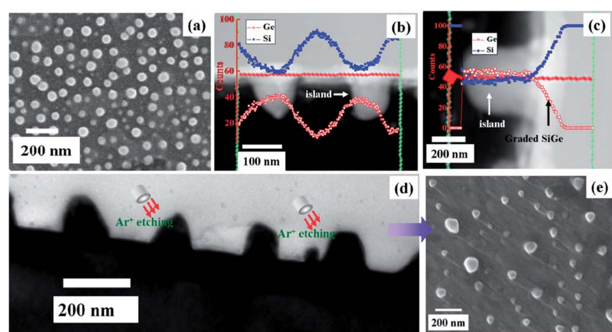

Fig. 3 Structures and composition of the fabricated SiGe islands and SiGe island/SiGe/Si nanowires. (a) SEM image of the island structures. (b) ADF-STEM image of the adjacent islands, and EDS line profile of Si and Ge through the adjacent islands. (c) ADF-STEM image of the islands, and line profile of the EDS signal from the Si and Ge components along the island growth axis. Beneath the uniform SiGe island, a 40 nm graded SiGe appears. The composition of the $Si_{1-x}Ge_x$ alloy island is estimated to be $Si_{0.7}Ge_{0.3}$, and the composition of the $Si_{1-x}Ge_x$ alloy in the free areas is $Si_{0.88}Ge_{0.12}$. (d) Cross-sectional TEM image of the structures of the islands. (e) SEM image of the SiGe island/SiGe/Si nanowires after Ar ion beam etching.

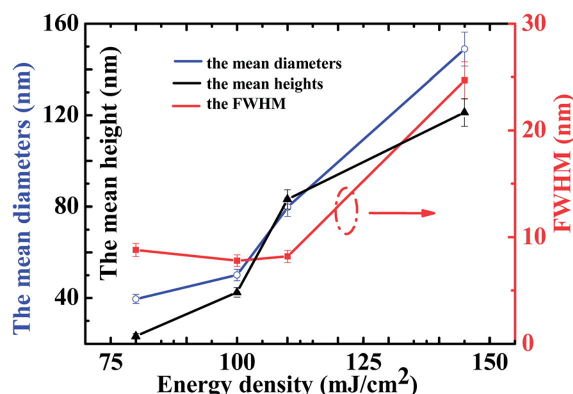

Fig. 4 The mean diameters, the mean height and the distribution full width at half maximum (FWHM) of SiGe islands with different laser energy densities: 80 mJ cm^{-2}, 100 mJ cm^{-2}, 110 mJ cm^{-2} and 145 mJ cm^{-2}. The mean diameters and the standard deviations, in nanometers (nm), were (39.6, 8.8), (50.1, 7.8), (79.8, 8.2) and (148.9, 24.7), respectively. The mean heights which were obtained from AFM images were 23.3 nm, 42.5, 83.2 and 121.2 nm, respectively.

 This journal is © The Royal Society of Chemistry 2013

Published on 04 September 2013. Downloaded by Xiamen University on 12/07/2015 08:24:29.

of Fig. 5 show SEM micrographs of SiGe islands with different laser energy densities. The diameters of the islands narrowly distributes when the energy density is below 145 mJ cm^{-2}. As the energy density increases to 145 mJ cm^{-2}, both large islands and small islands exist, and the shape of the islands tends to be asymmetric, as shown in Fig. 5(d). In this situation, we estimate the condition on the surface exposure corresponds to the melting when surface tension is driving the formation of droplet-like morphology on the surface.

As a comparative experiment, isolated SiGe islands with various diameters were used as masks in the Ar IBE of a Si (110) substrate. In Fig. 5(e), the top SiGe islands almost disappear and the NWs were no longer obvious after etching. In Fig. 5(f), although some of the top SiGe islands also disappear, the shape of the NWs is better than in Fig. 5(e). Interestingly, the images of Fig. 5(g)–(h) show the presence of the SiGe tips, demonstrating the blocking effect of the tip islands. The orientation of the etched NWs is perfect, which corresponds to the incidence angle of the Ar ion beam. Furthermore the SEM images of the NWs also show a good match of the wire arrangement with the islands. Fig. 6 is the evolution process of the SiGe island/SiGe/Si nanowires after Ar ion beam etching. At the beginning of the etching, the top islands can act as a mask. As the etching time continues, the size of the islands becomes small, and which can also act as masks. If the etching time is too long, the islands are also etched, ultimately resulting in the unobvious NWs, like Fig. 6(d). The low energy laser induces islands with a small diameter (40 nm), which may result in islands with a low height. With the increase of the laser energy, the size of the islands becomes larger, and perfect hetero-nanowires can be formed, since the size of the as-synthesized nanowire depends strongly on the diameter of the masking SiGe islands. The Ar ion beam etching rate for Si and Ge is different,[42–44] but if the height of the AR of islands is low, these islands cannot be seen as masks and can also be etched after ion beam etching technique. From the above analysis we know that high Ge content SiGe islands can act as masks because the ion beam etching rate is low, and ultimately these hetero-nanowire structures are formed. This opens up a whole new window for Si-based nanostructures with small feature sizes and complicated design patterns that could be of great importance for Si based nanodevices.

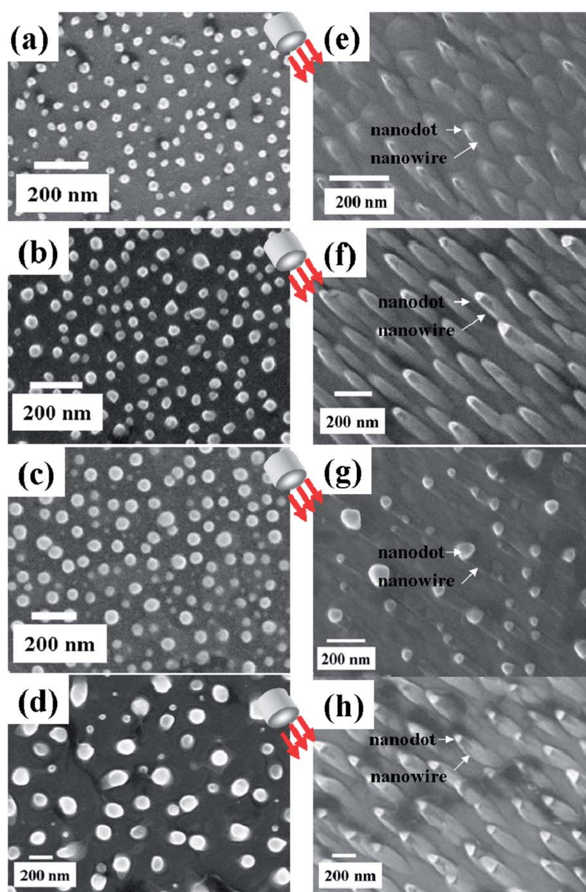

Fig. 5 SEM images of the SiGe islands with average diameters of (a) 39.6 nm, (b) 50.1 nm, (c) 79.8 nm and (d) 148.9 nm. (e) to (h) show the corresponding SiGe island/SiGe/Si NWs produced from (a) to (d).

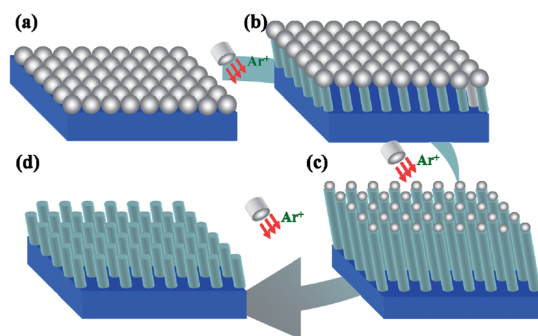

Fig. 6 Evolution process of SiGe island/SiGe/Si nanowires after Ar ion beam etching.

4. Conclusions

In conclusion, laser-induced SiGe islands can be used as masks to fabricate hetro-nanowires. The islands of high AR, as large as 0.96, enabled them to survive the Ar ion beam etching, and then ultimately formed SiGe island/SiGe/Si NWs with diameters ranging from 39.6 to 148.9 nm, and up to 10^9 wires per cm^2 in density. The direction of the nanowires was controlled by the beam incidence and the diameter of the nanowires was controlled by the annealing laser energy densities. The above processes provide an effective method to prepare catalyst-free Si-based nanowire structures, which could be well applied in future nanoelectronic and optoelectronic devices.

Acknowledgements

This work is supported by the National Natural Science Foundation of China under Grant no. 61176050, 61036003, and 61176092. The Fundamental Research Funds for the Fujian province of China no. 2012H0038. The National Basic Research Program of China under Grant no. 2012CB933503, no. 2013CB632103 and the Fundamental Research Funds for the Central Universities (2010121056).

Published on 04 September 2013. Downloaded by Xiamen University on 12/07/2015 08:24:29.

Notes and references

1 Y. Cui and C. M. Lieber, *Science*, 2001, **291**, 851.
2 J. Chen, *J. Mater. Chem.*, 2007, **17**, 4639.
3 V. Schmidt, H. Riel, S. Senz, S. Karg, W. Riess and U. Gösele, *Small*, 2006, **2**, 85–88.
4 J. Wu, M. Wieligor, T. W. Zerda and J. L. Coffer, *Nanoscale*, 2010, **2**, 2657.
5 M. H. Huang, F. Cavallo, F. Liu and M. G. Lagally, *Nanoscale*, 2011, **3**, 96.
6 B. Tian, X. Zheng, T. J. Kempa, Y. Fang, N. Yu, G. Yu, J. Huang and C. M. Lieber, *Nature*, 2007, **449**, 885–890.
7 L. Li, T. Zhai, H. Zeng, X. Fang, Y. Bando and D. Golberg, *J. Mater. Chem.*, 2011, **21**, 40.
8 F. Patolsky, G. Zheng and C. M. Lieber, *Nat. Protoc.*, 2006, **1**, 1711–1724.
9 M. Yu, Y. Z. Long, B. Sun and Z. Y. Fan, *Nanoscale*, 2012, **4**, 2783.
10 Z. P. Huang, N. Geyer, P. Werner, J. D. Boor and U. Gösele, *Adv. Mater.*, 2011, **23**, 285–308.
11 C. L. Lee, K. Tsujino, Y. Kanda, S. Ikeda and M. Matsumura, *J. Mater. Chem.*, 2008, **18**, 1015.
12 N. Geyer, Z. P. Huang, B. Fuhrmann, S. Grimm, M. Reiche, T. K. Nguyen-Duc, J. D. Boor, H. S. Leipner, P. Werner and U. Gösele, *Nano Lett.*, 2009, **9**, 3106–3110.
13 K. Q. Peng, M. L. Zhang, A. J. Lu, N. B. Wong, R. Q. Zhang, *et al.*, *Appl. Phys. Lett.*, 2007, **90**, 163123.
14 A. I. Hochbaum, R. Fan, R. R. He and P. D. Yang, *Nano Lett.*, 2005, **5**, 457.
15 J. Goldberger, A. Hochbaum, R. Fan and P. D. Yang, *Nano Lett.*, 2006, **6**, 973.
16 R. R. He, R. Fan, A. I. Hochbaum, C. Carraro, R. Maboudian and P. D. Yang, *Adv. Mater.*, 2005, **17**, 2098.
17 Y. Y. Wu and P. D. Yang, *J. Am. Chem. Soc.*, 2001, **123**, 3165.
18 H. F. Yan, Y. J. Xing, Q. L. Hang, D. P. Yu, Y. P. Wang, J. Xu, Z. H. Xi and S. Q. Feng, *Chem. Phys. Lett.*, 2000, **323**, 224.
19 R. Q. Zhang, Y. Lifshitz and S. T. Lee, *Adv. Mater.*, 2003, **15**, 635.
20 Y. Wang, V. Schmidt, S. Senz and U. Gösele, *Nat. Nanotechnol.*, 2006, **1**, 186.
21 S. P. Ge, K. L. Jiang, X. X. Lu, Y. F. Chen, R. M. Wang and S. S. Fan, *Adv. Mater.*, 2005, **17**, 56.
22 J. D. Holmes, K. P. Johnston, R. C. Doty and B. A. Korgel, *Science*, 2000, **287**, 1471.
23 K. Q. Peng, A. J. Lu, R. Q. Zhang and S. T. Lee, *Adv. Funct. Mater.*, 2008, **18**, 3026–3035.
24 P. Gorostiza, R. Diaz, J. Servat, F. Sanz and J. R. Morante, *J. Electrochem. Soc.*, 1997, **144**, 909.
25 H. Morinaga, M. Suyama and T. Ohmi, *J. Electrochem. Soc.*, 1994, **141**, 2834.
26 N. Mitsugi and K. Nagai, *J. Electrochem. Soc.*, 2004, **151**, G302.
27 D. P. Divincenzo, *Science*, 1995, **270**, 255.
28 W. Porod, C. S. Lent, G. H. Bernstein, A. O. Orlov, I. Amlani, G. L. Snider and J. L. Merz, *Int. J. Electron.*, 1999, **86**, 549.
29 S. S. Li, G. L. Long, F. S. Bai, S. L. Feng and H. Z. Zheng, *Proc. Natl. Acad. Sci. U. S. A.*, 2001, **98**, 11847.
30 G. Burkard, D. Loss and D. P. DiVincenzo, *Phys. Rev. B: Condens. Matter Mater. Phys.*, 1999, **59**, 2070.
31 O. Leifeld, A. Beyer, E. Muller, D. Grutzmacher and K. Kern, *Thin Solid Films*, 2000, **380**, 176.
32 J. Y. Kim, S. H. Ihm, J. H. Seok, C. H. Lee, E. K. Suh and H. J. Lee, *Thin Solid Films*, 2000, **369**, 96.
33 Y. Wakayama, G. Gerth, P. Werner and L. V. Sokolov, *Surf. Sci.*, 2001, **493**, 399.
34 D. J. Eaglesham and M. Cerullo, *Phys. Rev. Lett.*, 1990, **64**, 1943.
35 Y. W. Mo, D. E. Savage, B. S. Swartzentruber and M. G. Lagally, *Phys. Rev. Lett.*, 1990, **65**, 1020.
36 R. G. Medeiros, A. M. Bratkovski, T. I. Kamins, D. A. A. Ohlberg and R. S. Williams, *Science*, 1998, **279**, 353.
37 M. Stoffel, A. Rastelli, J. Tersoff, T. Merdzhanova and O. G. Schmidt, *Phys. Rev. B: Condens. Matter Mater. Phys.*, 2006, **74**, 155326.
38 M. Brehm, H. Lichtenberger, T. Fromherz and G. Springholz, *Nanoscale Res. Lett.*, 2011, **6**, 70.
39 X. G. Peng, L. Manna, W. D. Yang, J. Wickham, E. Scher, A. Kadavanich and A. P. Alivisatos, *Nature*, 2000, **404**, 59.
40 Y. Nakamura1, A. Masada and M. Ichikawa, *Appl. Phys. Lett.*, 2007, **91**, 013109.
41 V. I. Klimov, A. A. Mikhailovsky, S. Xu, A. Malko, J. A. Hollingsworth, C. A. Leatherdale, H.-J. Eisler and M. G. Bawendi, *Science*, 2000, **290**, 314.
42 Y. Wang and N. Herron, *J. Phys. Chem.*, 1991, **95**(2), 525.
43 T.-W. Kim, *Appl. Phys. Lett.*, 2006, **88**(12), 12302.
44 T. Takagahara and K. Takeda, *Phys. Rev. B: Condens. Matter*, 1992, **46**, 15578.
45 Y. B. Hahn, D. C. Hays, S. M. Donovan, C. R. Abernathy, J. Han, R. J. Shul, H. Cho, K. B. Jung and S. J. Pearton, *J. Vac. Sci. Technol., A*, 1999, **17**, 768.
46 H. S. Kim, G. Y. Yeom, J. W. Lee and T. I. Kim, *Thin Solid Films*, 1999, **341**, 180.
47 H. F. Winters and J. W. Coburn, *Surf. Sci. Rep.*, 1992, **14**, 261.
48 J. W. Coburn and H. F. Winters, *J. Vac. Sci. Technol.*, 1979, **16**, 391.
49 H. F. Winters, *J. Vac. Sci. Technol., A*, 1988, **6**, 1997.
50 W. X. Chen, L. M. Walpita, C. C. Sun and W. S. C. Chang, *J. Vac. Sci. Technol., B*, 1986, **4**, 701.
51 A. Sinitski, S. Neumeier, J. Nelles, M. Fischler and U. Simon, *Nanotechnology*, 2007, **18**, 305307.
52 K. J. Morton, G. Nieberg, S. Bai and S. Y. Chou, *Nanotechnology*, 2008, **19**, 345301.
53 J. Q. Huang, S. Y. Chiam, H. H. Tan, S. J. Wang and W. K. Chim, *Chem. Mater.*, 2010, **22**, 4111.

This journal is © The Royal Society of Chemistry 2013